

Flexible cefalexin-immobilized graphene oxide film for antibacterial and drug delivery

Xun Xu, Fangwang Ming, Jinqing Hong, Zhoucheng Wang*

Department of Chemical and Biochemical Engineering, College of Chemistry and Chemical Engineering, Xiamen University, Xiamen, China

*Corresponding author, Tel: (+86) 18059217473; Fax: (+46) 5912180738; E-mail: zcwag@xmu.edu.cn

Received: 13 September 2016, Revised: 26 October 2016 and Accepted: 20 November 2016

DOI: 10.5185/amlett.2017.7103
www.vbripress.com/aml

Abstract

The flexible and freestanding graphene oxide (GO) film was fabricated for drug delivery and antibacterial. The film was synthesized by covalently attaching cefalexin onto graphene oxide sheets and then made by filtration of the colloidal suspension. SEM and optical images show that the Cefalexin-grafted graphene oxide (GO-CE) film possesses the unique 2D layer-by-layer structure and it could form channels for drug release when immersed in water. The drug loading and release tests certify that the GO-CE film is a promising drug delivery membrane with high load capacity (0.621 mg mg^{-1}) and long-acting release properties (72 h), and can effectively inhibit the growth of *E. coli* and *S. aureus* bacteria while showing minimal cytotoxicity for a long time. The cellular culture results of the HeLa Cells indicate that the GO-CE film exhibits excellent biocompatibility. Based on these advantages, the GO-CE film is expected to be used in the environmental and medical applications. Copyright © 2017 VBRI Press.

Keywords: Graphene oxide, chemical synthesis, thin films, antibacterial, drug delivery.

Introduction

Graphene, a unique carbon material comprises two-dimensional one-atom-thick carbon atoms hexagonally arranged into a 2D structure [1-3]. It has become one of the most attractive function materials in some areas because of its brilliant mechanical and electrical properties [1, 4-6]. Graphene oxide (GO), an important derivative of graphene, has inherited some unique properties from graphene. Additionally, it contains plentiful kinds of functional groups, such as hydroxyl, carboxyl, epoxide and carbonyl groups on its surfaces [7, 8]. Due to the functionalized surfaces, water-solubility and high specific surface area, GO and its derivatives have been researched as potential biological materials in recent years [8, 9].

It has been proved that GO is an effective absorbent material for several kinds of drugs [10-13]. These drug molecules strongly deposited onto GO surface via interaction, π - π bonding and cation- π bonding [10, 14]. Hence, GO is a potential material to establish a novel and efficient drug delivery system. So far, researchers have developed a large amount of drug delivery systems based on GO and its derivatives [8, 15-22]. In some researches, some functional polymer is grafted onto the GO sheet to improve its properties, such as solubility [15, 16, 23], biocompatibility and interfacial interactivity for specific drug [17, 18, 24]. Several forms of GO-based drug delivery systems have been explored to fit different situations, such as GO-polymer hybrid pills and membranes [18, 25-29], hydrogels [19, 30], and water soluble particles [25, 31-34].

The free standing and highly flexible GO film could be easily prepared by flow-directed assembly of individual GO sheets [35]. It has shown better mechanical strength, electrical properties and chemical activity than many other film-like materials [35, 36]. In some previously research, GO film has been proved to be a biocompatible substrate for adhesion and proliferation of several kind of human cells [37-39]. Thus, it is attractive to develop a new drug delivery film based on the GO film. However, so far as we know, few studies have been reported [40, 41].

Herein, we reported a simple way to fabrication of a flexible and drug-loaded GO film for antibacterial materials. Cefalexin, a commonly-used antibiotic, was chosen as the model drug and grafted onto the GO surface via amide linkage. The results demonstrate that Cefalexin, which is a bactericidal antibiotic widely used for the treatment of bacterial infections, can be released from Cefalexin-grafted GO (GO-CE) film and the sandwich structure of GO film provides adsorption space for the drug. Furthermore, the antibacterial test results show that hybrid films can inhibit bacterial growth for 48 hours. This work makes it possible for the first time to directly use GO-CE hybrid materials with antibacterial activity in drug delivery, and may facilitate the development of biological applications of GO-CE hybrid materials.

Experimental

Materials details

Graphite powder (1000 mesh) was purchased from Qingdao Chenyang graphite Co. Ltd (Tsingtao, China).

Cefalexin monohydrate (99%), N-(3-dimethylaminopropyl)-N'-ethylcarbodiimide hydrochloride (EDC·HCl, 99%), N-hydroxysuccinimide (NHS, 98.5%) and 3-(4,5-dimethylthiazol-2-yl)-2,5-diphenyltetrazolium Bromide (MTT, 99.5%) were obtained from Sigma Aldrich and used as received. Other chemicals are products of Sinopharm Chemical Reagent Co., Ltd (Shanghai, China). Deionized water was used throughout the experiment.

Synthesis of GO

GO was prepared by a modified Hummers method [42, 43]. In a typical synthesis process, 9:1 mixture of concentrated H_2SO_4 / H_3PO_4 (180/20 mL) solution was added to a 250 mL flask containing 1.5 g of graphite and 4.5 g of KMnO_4 at room temperature. Then the flask was heated to 50 °C in an oil-bath for 15 h. After that, 150 g ice was added into the resulting suspension to dilute the solution and 2 mL H_2O_2 (30 wt%) was injected. Then the reaction product was washed twice by 100 mL HCl (10 wt%). The remaining GO suspension was washed several times until the pH of GO suspension was above 6. Then the GO suspension was freeze-dried to obtain the final product. Morphologies of GO sheets were shown in Fig. S1†.

Synthesis of GO-CE film

The GO-CE films were synthesized by covalent linking of the carboxyl ($-\text{COOH}$) groups of GO with the amino ($-\text{NH}_2$) groups of cefalexin molecule. The carboxyl groups of GO were activated using EDC and NHS [19]. Briefly, GO (100 mg) was dispersed in a 100 mL solution of phosphate buffer solution (PBS) (0.1 M, pH adjusted to 5.5). The mixture was sonicated for 30 min to obtain an homogeneous colloidal suspension. Then EDC·HCl (1 g) and NHS (0.2 g) were gradually added into the suspension and reaction for 20 min. Afterwards, various amounts of cefalexin monohydrate was added into the suspension and sonicated for 30 min. The reaction was continued at 37 °C in an oil-bath under vigorous stirring for 24 h. When the reaction was terminated, the resultant was separated from water via centrifugal separation. Then the resultant was washed several times with a large amount of deionized water. Then the products were freeze-dried to obtain GO-CE sheets.

Free-standing flexible GO-CE film was prepared by vacuum assisted flow-filtration method. Typically, GO-CE (0.1 g) sheets were dispersed in 20 mL solution of PBS (0.05 M, pH adjusted to 7.4). The mixture was sonicated for 60 min to obtain a homogeneous colloidal suspension. Then the GO-CE film was made by filtration of the colloidal suspension using a cellulose acetate membrane filter membrane (47 mm in diameter, 0.45 μm pore size). The GO-CE film samples were vacuum-dried at room temperature before subsequent tests. GO film was prepared by the same method.

Characterizations

X-ray diffraction (XRD) of all the prepared materials were performed on a Rigaku Ultima IV diffraction

instrument (Rigaku Co., Japan) using a Cu tube as X-ray source ($\lambda_{\text{Cu K}\alpha} = 1.54 \text{ \AA}$) a tube voltage of 35 kV and a current of 35 mA. The morphologies of the samples were characterized by scanning electronic microscopy (SEM) using a Zeiss SIGMA microscope (Germany). Attenuation reflectance Fourier transformation infrared spectrometry (ATR-FTIR) spectra were collected on an Avatar 360 infrared spectro-photometer (America).

Results and discussion

As show in the photographs (fig. 1a and b), both GO and GO-CE films are free-standing and flexible. Individual GO sheets within the film form continuous networks via layer folding and Vander Waals force which providing good flexibility and mechanical integrity [38, 44]. The colour of GO-CE film (Fig. 1b) is darkened and tarnish compared with the brown GO film (fig. 1a) indicated that a restore of the π -electron system in the GO sheets [45]. The flexibility and mechanical integrity of GO-CE film suggest its applicability for varied fields such as food packaging and biomaterial. The surface profiles of the GO and GO-CE films are observed by SEM and were displayed in Fig. 1 c-f. It could be found from the SEM images that the surface of GO film (Fig. 1c, d) is flatter than that of GO-CE film (Fig. 1e, f). More wrinkles both on the micro- and macro-scopic scales are also observed on the GO-CE film. The formations of wrinkles on the GO and GO-CE films are related to the hydrogen bond interactions between the adjacent GO.

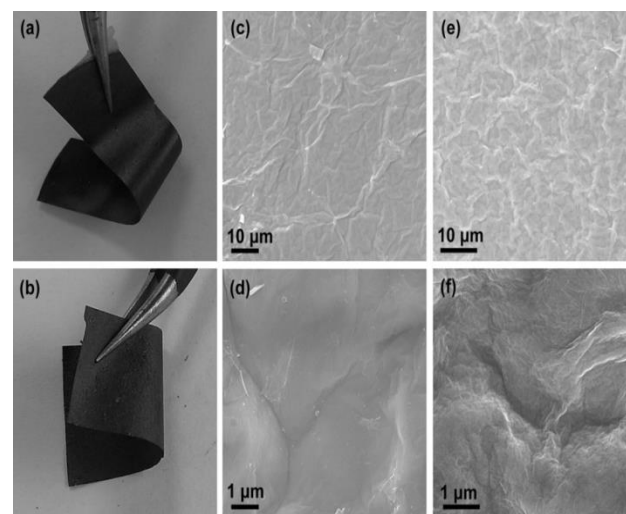


Fig. 1. Photographs of free-standing film samples: GO (a) and GO-CE (b); SEM images of surface morphology of GO film (c) and (d), GO-CE film (e) and (f) (All samples were Pt coated to improve the electrical conductivity before test).

Fig. 2 shows the ATR-FTIR spectra of GO film, GO-CE film and cefalexin monohydrate powders. ATR-FTIR spectroscopy of GO film reveals that several kinds of functional groups are formed on the surface of GO film. The most characteristic features are the adsorption bands corresponding to $\text{C}=\text{O}$ carbonyl stretching at 1734 cm^{-1} , $\text{C}=\text{C}$ skeletal vibrations of unoxidized graphite domains at 1629 cm^{-1} , $\text{C}-\text{OH}$ stretching at 1208 cm^{-1} , $\text{C}-\text{O}$ stretching (epoxy or alkoxy) at 1041 cm^{-1} and ubiquitous $\text{O}-\text{H}$ stretches appear at $2800\sim 3700 \text{ cm}^{-1}$ [46-48].

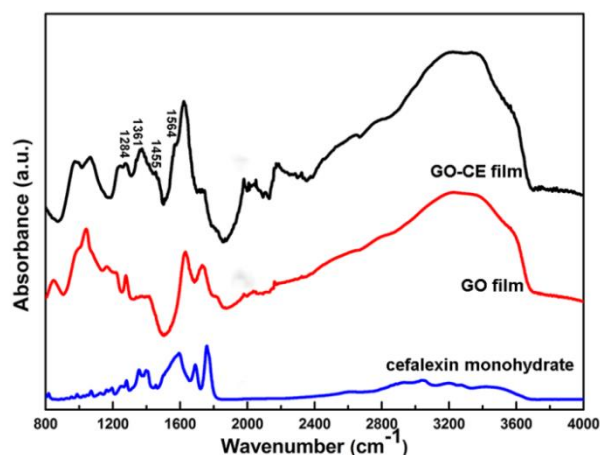


Fig. 2. ATR-FTIR spectra of GO-CE film, GO film, and cefalexin monohydrate powders.

Several new peaks appear on the FTIR spectrum of GO-CE film in comparison with the GO film's spectrum. The characteristic of amide ($-\text{C}(\text{O})\text{NH}-$) stretching vibration at 1564 cm^{-1} indicates the presence of the amide bond formed by reaction between GO and cefalexin molecule. Moreover, there are also a few characteristic peaks of cefalexin molecule appeared in the GO-CE film. The bands at 1361 and 1455 cm^{-1} represent C-H bending vibrations and the band at 1284 cm^{-1} represents C-N stretching vibrations in cefalexin [49]. These results indicate that cefalexin molecules were grafted onto the GO surface during the experiment [50]. The quantified atom fraction of the elements C, O, N and S found in the surface composition of the GO and GO-CE films is shown in **Table 1**. The oxygen content reduced from 40.15 at.% for GO film to 32.50 at.% for GO-CE film and the corresponding O/C ratio decreases from 0.685 to 0.524 as well. What is more, the nitrogen content in GO-CE film is 4.6 at.%, while it is not detected in GO film. The result of element content further confirms the conclusion of ATR-FTIR spectra analysis.

Table 1. EDS analysis of element content and calculated C/O and C/N ratios for GO and GO-CE film samples.

Sample	C (at. %)	O (at. %)	N (at. %)	S (at. %)	Organic groups	Nitrogen groups
GO paper	58.5 9	40.1 5	0	1.26	COOH	None
GO- CE paper	62.0 0	32.5 0	4.62	0.63	COOH, diisocya nate	amino, cefalexin

SEM images of the cross section of GO-CE film (**Fig. 3d**) reveal the well-packed layers in a 2D layer-by-layer hierarchy. It can be seen from the cross section that most of the GO sheets pack tightly in an ordered fashion. Only few elongated gaps could be seen on the cross section because of the debonded GO sheets or bundles [51]. However, apparent gaps (about $0.5\sim 1.5\text{ }\mu\text{m}$) could be observed in the cross section of water-swollen GO-CE film (**Fig. 3e**), which is attributed to the separation and "corrosion" of the graphene oxide sheets by the water. As

shown in **Fig. 3a-c**, the film would be swollen when soak in PBS solution. The appearance of gaps in the water-swollen sample might act as a "release channel" for drug release.

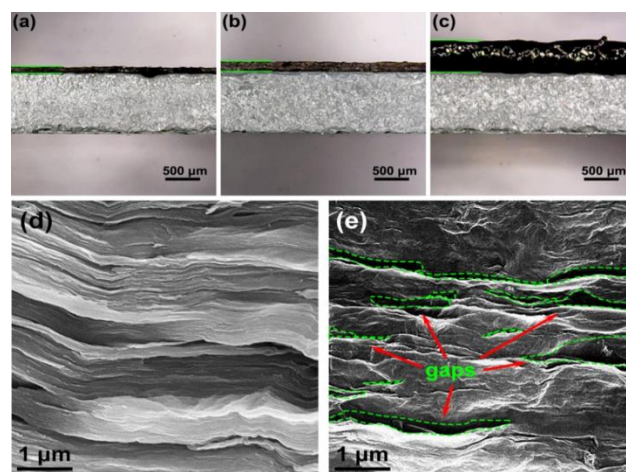


Fig. 3. The images of GO-CE film's side face thickness increase when soaked in PBS (pH=7.4). Primitive thickness (a), after 1 h (b), after 24 h (c); SEM images of cross section of GO-CE film (d) and water-swollen sample of the same film (f).

Earlier studies had found two common routes for small molecules to adsorb on the surface of GO sheets. For one thing, some small molecules with aromatic group could adsorb on the surface of GO sheets with the help of Van der Waals force between them [12, 13, 15, 20, 27]. The other routes were chemical interaction between carboxyl groups in GO and functional groups in drug molecules [8, 16, 18, 22]. The loading capacity of cefalexin on GO was determined by UV spectrum, and was calculated by the difference of cefalexin concentrations between the initial solution and the supernatant solution after reaction. The loading of cefalexin on GO is shown in **Fig. 4a**.

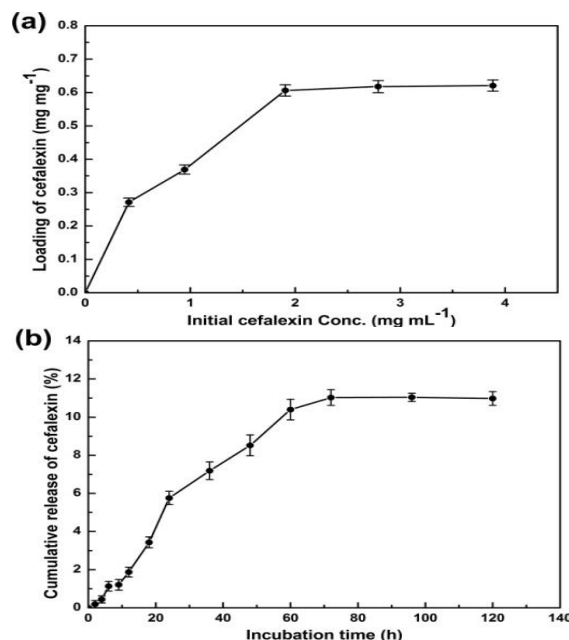


Fig. 4. Loading capacity of cefalexin on GO in different initial concentrations (a), the release of cefalexin on GO-CE film in PBS solution (pH=7.4) (b)

The saturated loading amount of cefalexin on GO is 0.621 mg mg^{-1} . **Fig. S3** and **Fig. 4b** shows the release profiles of cefalexin molecules from GO-CE film in PBS solution ($\text{pH} = 7.4$), in comparison with those from the free GO-CE particles. It can also be observed that the GO-CE films exhibited a longer release time than the free GO-CE particles. Moreover, on the basis of the release profile, the equilibrium percentage of released cefalexin molecules was not as high as 100% (11% for GO-CE films and 92% for GO-CE particles), which is due to the characteristics of the ion-exchange reaction. The ion-exchange reaction is an equilibrium process, thus the interlayer molecules cannot be exchanged completely [54, 56]. The results revealed that the combination of cefalexin with GO to form a sandwich structure film could help to prolong the release time and most of the cefalexin (about 89%) was adsorbed on the interlayer space. The swelling property of the GO-CE film reveals an important factor in drug process as well. Water molecules could intrude into 2D layer-by-layer GO sheets and separate the adjacent nanosheets when GO-CE film was water-swollen. Hence, cefalexin molecules adsorbed on GO surface could find a way to dissolve in water and release from the membrane.

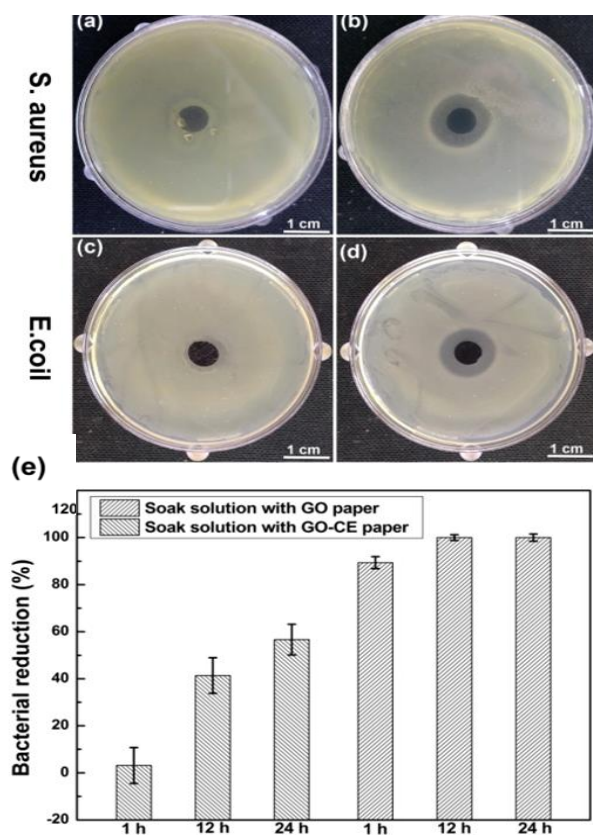


Fig. 5. The antibacterial inhibition zone of GO film (a) and (c), GO-CE film (b) and (d). Reduction in the bacteria colonies as an index of bacteriostasis ability for each drug release solution (e).

Antibacterial activity of GO and GO-CE films against *S. aureus* and *E. coli* are shown in **Fig. 5**. It can be seen that the inhibition zone generated by GO film was obscure and tiny. The GO suspension liquid with excellent antibacterial ability had been confirmed in some previous studies [39, 52]. However, the antibacterial

ability was weakened when GO floccled together to form particles or films [39, 53], since it is hard for dissociative GO nanosheets to “escape” from an orderly and compact tissues. The antibacterial ability of GO-CE film achieves significant improvement by the addition of cefalexin. The GO-CE disks produce clearness zones of inhibition against *S. aureus* ($r = 0.69 \text{ cm}$) and *E. coli* ($r = 0.63 \text{ cm}$) (fig. 5b and d). The release of cefalexin exhibits an excellent bactericidal ability as compared with the GO sample. Bacterial reduction for the immersion fluid of GO and GO-CE film also validates the previous result (**Fig. 5d**). The bacterial reduction bar graph reveals that the antibacterial effect of GO-CE film is effective rapidly (1 h for 89.375% bacterial reduction) and the antibacterial effect could sustain for a long time (24 h for almost 100% bacterial reduction). The GO-CE film has shown better antibacterial activity as compared to other GO related antibacterial material (**Table S1**), suggesting that GO-CE film is a very hopeful antibacterial material. The reason for the efficiency inhibition of bacterial growth may be due to the following factors. First, GO could induced cellular damage of *S. aureus* and *E. coli* from the effects of oxidative stress and physical disruption [36]. Secondly, the combined effect of antibacterial activity of GO and cefalexin released from GO-CE paper [19].

The results of MTT assay for the GO and GO-CE suspension are summarized in **Fig. 6**. As indicated in **Fig. 6a**, there is no obvious toxicity ($>80\%$ cell viability) for GO and GO-CE suspension after 72 h, even at a high concentration of $50 \mu\text{g mL}^{-1}$ for HeLa Cells. Since little GO-CE sheets could peel off from GO-CE when soaked in the water, it is seen that the GO-CE film is an antibacterial materials with mild cytotoxicity.

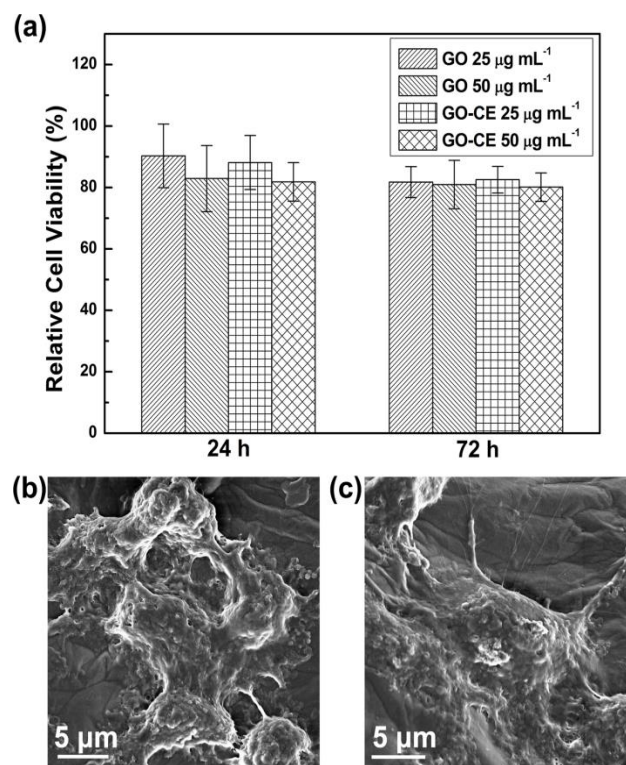


Fig. 6. Relative cell viability of HeLa cells treated with GO and GO-CE at various concentrations (a), SEM morphologies of the HeLa cells cultured on the surface of GO (b) and GO-CE (c) films for 24 h.

The morphologies of HeLa Cells cultured on the GO and GO-CE films were studied by SEM (**Fig. 6b, c**). From the SEM images, HeLa cells show a large spreading area and the cell-substrate boundary is hardly distinguishable, in addition, pseudopodias are formed in the edge of cells (**Fig. 6c**). The morphology of the HeLa cells indicates that HeLa cells grow well and adhere tightly on the GO-CE film. This association may be attributed to the synergistic effects of the reactive hydrophilic groups and the increase of surface wrinkles of GO-CE film [59].

Conclusion

In this work, a flexible and free-standing antibacterial film is prepared via a simple way based on the cefalexin-grafted GO nanosheets. The GO-CE film possesses a unique 2D layer-by-layer structure and the sandwich structure of GO film provides adsorption space for the drug. The drug release behavior of GO-CE film suggests a dramatic increase of effective release time. Additionally, GO-CE film exhibits a high-efficiency antibacterial effect with favorable biocompatibility. The novel film structures, combined with multi-functionalities including biocompatibility, drug loading and delivery, and antibacterial activities, suggest promising applications of this kind of hybrid material in biological and medical areas.

Acknowledgements

The authors would like to thank the National Natural Science Foundation of China (51372212).


Author's contributions

Conceived the plan: zcw; Performed the experiments: xx; Data analysis: xx, fwm, jqh; Wrote the paper: xx, zcw. Authors have no competing financial interests.

References

- Novoselov, K.S.; Geim, A.K.; Morozo, S.; Jiang D.; Zhang Y.; Dubonos S.; Grigorieva I.; Firsov A.; *Science* **2004**, *306*, 666. DOI: [10.1126/science.1102896](https://doi.org/10.1126/science.1102896)
- Geim, A.K.; Novoselov, K.S.; *Nat. Mater.*, **2007**, *6*, 183. DOI: [10.1038/nmat1849](https://doi.org/10.1038/nmat1849)
- Rao, C. N. R.; Sood, A. K.; Subrahmanyam, K. S.; Govindaraj, A.; *Angew. Chem., Int. Ed.*, **2009**, *48*, 7752. DOI: [10.1002/anie.200901678](https://doi.org/10.1002/anie.200901678)
- Lee, C.; Wei, X.; Kysar, J.W.; Hone, J.; *Science* **2008**, *321*, 385. DOI: [10.1126/science.1157996](https://doi.org/10.1126/science.1157996)
- Stankovich, S.; Dikin, D.A.; Dommett, G.H.; Kohlhaas, K.M.; Zimney, E.J.; Stach, E.A.; Piner, R.D.; Nguyen, S.T.; Ruoff, R.S.; *Nature* **2006**, *442*, 282. DOI: [10.1038/nature04969](https://doi.org/10.1038/nature04969)
- Zhang, Y.; Tan, Y.-W.; Stormer, H.L.; Kim, P.; *Nature* **2005**, *438*, 201. DOI: [10.1038/nature04235](https://doi.org/10.1038/nature04235)
- Zhu, Y.; Murali, S.; Cai, W.; Li, X.; Suk, J. W.; Potts, J. R.; Ruoff, R. S.; *Adv. Mater.*, **2010**, *22*, 3906. DOI: [10.1002/adma.201001068](https://doi.org/10.1002/adma.201001068)
- Sun, X.; Liu, Z.; Welsher, K.; Robinson, J.T.; Goodwin, A.; Zaric, S.; Dai, H.; *Nano Res.*, **2008**, *1*, 203. DOI: [10.1007/s12274-008-8021-8](https://doi.org/10.1007/s12274-008-8021-8)
- Ma, X.; Tao, H.; Yang, K.; Feng, L.; Cheng, L.; Shi, X.; Li, Y.; Guo, L.; Liu, Z.; *Nano Res.*, **2012**, *5*, 199. DOI: [10.1007/s12274-012-0200-y](https://doi.org/10.1007/s12274-012-0200-y)
- Gao, Y.; Li, Y.; Zhang, L.; Huang, H.; Hu, J.; Shah, S.M.; Su, X.; *J. Colloid Interface Sci.*, **2012**, *368*, 540. DOI: [10.1016/j.jcis.2011.11.015](https://doi.org/10.1016/j.jcis.2011.11.015)
- Tang, Y.; Guo, H.; Xiao, L.; Yu, S.; Gao, N.; Wang, Y.; *Colloids Surf., A* **2013**, *424*, 7. DOI: [10.1016/j.colsurfa.2013.02.030](https://doi.org/10.1016/j.colsurfa.2013.02.030)
- Lin, Y.; Xu, S.; Li, J.; *Chem. Eng. J.*, **2013**, *225*, 679. DOI: [10.1016/j.cej.2013.03.104](https://doi.org/10.1016/j.cej.2013.03.104)
- Chen, H.; Gao, B.; Li, H.; *J. Hazard. Mater.*, **2015**, *282*, 201. DOI: [10.1016/j.jhazmat.2014.03.063](https://doi.org/10.1016/j.jhazmat.2014.03.063)
- Qi, X.; Gunawan, P.; Xu, R.; Chang, M.W.; *Chem. Eng. Sci.*, **2012**, *84*, 552. DOI: [10.1016/j.ces.2012.08.054](https://doi.org/10.1016/j.ces.2012.08.054)
- Bao, H.; Pan, Y.; Ping, Y.; Sahoo, N.G.; Wu, T.; Li, L.; Li, J.; Gan, L.H.; *Small* **2011**, *7*, 1569. DOI: [10.1002/smll.201100191](https://doi.org/10.1002/smll.201100191)
- Shan, C.; Yang, H.; Han, D.; Zhang, Q.; Ivaska, A.; Niu, L.; *Langmuir* **2009**, *25*, 12030. DOI: [10.1021/la903265p](https://doi.org/10.1021/la903265p)
- Liu, J.; Cui, L.; Losic, D.; *Acta Biomater.*, **2013**, *9*, 9243. DOI: [10.1016/j.actbio.2013.08.016](https://doi.org/10.1016/j.actbio.2013.08.016)
- Gao, J.; Bao, F.; Feng, L.; Shen, K.; Zhu, Q.; Wang, D.; Chen, T.; Ma, R.; Yan, C.; *RSC Adv.*, **2011**, *1*, 1737. DOI: [10.1039/C1RA00029B](https://doi.org/10.1039/C1RA00029B)
- Tao C.-a.; Wang, J.; Qin, S.; Lv, Y.; Long, Y.; Zhu, H.; Jiang, Z.; *J. Mater. Chem.*, **2012**, *22*, 24856. DOI: [10.1039/C2JM34461K](https://doi.org/10.1039/C2JM34461K)
- Tiwari, A.; (Eds), *In the Graphene materials: Fundamentals and emerging applications*, John Wiley & Sons, USA, **2015**.
- Depan, D.; Shah, J.; Misra, R.; *Mater. Sci. Eng., C* **2011**, *31*, 1305. DOI: [10.1016/j.msec.2011.04.010](https://doi.org/10.1016/j.msec.2011.04.010)
- Fan, X.; Jiao, G.; Zhao, W.; Jin, P.; Li, X.; *Nanoscale*, **2013**, *5*, 1143. DOI: [10.1039/C2NR33158F](https://doi.org/10.1039/C2NR33158F)
- Zhang, Q.; Wu, S.; Zhang, L.; Lu, J.; Verproot, F.; Liu, Y.; Xing, Z.; J. Li, Song, X.-M.; *Biosens. Bioelectron.*, **2011**, *26*, 2632. DOI: [10.1016/j.bios.2010.11.024](https://doi.org/10.1016/j.bios.2010.11.024)
- Rana, V.K.; Choi, M.C.; Kong, J.Y.; Kim, G.Y.; Kim, M.J.; Kim, S.H.; Mishra, S.; Singh, R.P.; Ha, C.S.; *Macromol. Mater. Eng.*, **2011**, *296*, 131. DOI: [10.1002/mame.201000307](https://doi.org/10.1002/mame.201000307)
- Liu, Q.; Shi, J.; Cheng, M.; Li, G.; Cao, D.; Jiang, G.; *Chem. Commun.*, **2012**, *48*, 1874. DOI: [10.1039/C2CC16891J](https://doi.org/10.1039/C2CC16891J)
- Justin, R.; Chen, B.; *Carbohydr. Polym.*, **2014**, *103*, 70. DOI: [10.1016/j.carbpol.2013.12.012](https://doi.org/10.1016/j.carbpol.2013.12.012)
- Sharon, M.; Sharon, M.; Shinohara, H.; Tiwari, A.; (Eds), *In the Graphene: An Introduction to the Fundamentals and Industrial Applications*, Wiley, USA, **2015**.
- Qi, W.; Xue, Z.; Yuan, W.; Wang, H.; *J. Mater. Chem. B* **2014**, *2*, 325. DOI: [10.1039/C3TB21387K](https://doi.org/10.1039/C3TB21387K)
- Huang, T.; Zhang, L.; Chen, H.; Gao, C.; *J. Mater. Chem. B* **2015**, *3*, 1605. DOI: [10.1039/c4tb01896f](https://doi.org/10.1039/c4tb01896f)
- Wang, H.; Sun, D.; Zhao, N.; Yang, X.; Shi, Y.; Li, J.; Su, Z.; Wei, G.; *J. Mater. Chem. B* **2014**, *2*, 1362. DOI: [10.1039/C3TB21538E](https://doi.org/10.1039/C3TB21538E)
- Ghosh, A.; Rao, K.V.; George, S.J.; Rao, C.; *Chem. Eur. J.*, **2010**, *16*, 2700. DOI: [10.1002/chem.200902828](https://doi.org/10.1002/chem.200902828)
- Zhang, L.; Xia, J.; Zhao, Q.; Liu, L.; Zhang, Z.; *Small* **2010**, *6*, 537. DOI: [10.1002/smll.200901680](https://doi.org/10.1002/smll.200901680)
- Tiwari, A.; Syväjärvi, M.; (Eds), *In Advanced 2D Materials*, John Wiley & Sons, Beverly, MA, USA, **2016**.
- Turcheniuk, K.; Hage, C.-H.; Spadavecchia, J.; Serrano, A.Y.; Larroulet, I.; Pesquera, A.; Zurutuza, A.; Pisfil, M.G.; Hélot, L.; Boukaert, J.; *J. Mater. Chem. B* **2015**, *3*, 375. DOI: [10.1039/C4TB01760A](https://doi.org/10.1039/C4TB01760A)
- Dikin, D.A.; Stankovich, S.; Zimney, E.J.; Piner, R.D.; Dommett, G.H.; Evmenenko, G.; Nguyen, S.T.; Ruoff, R.S.; *Nature* **2007**, *448*, 457. DOI: [10.1038/nature06016](https://doi.org/10.1038/nature06016)
- Park, S.; Lee, K.-S.; Bozoklu, G.; Cai, W.; Nguyen, S.T.; Ruoff, R.S.; *ACS nano* **2008**, *2*, 572. DOI: [10.1021/nn700349a](https://doi.org/10.1021/nn700349a)
- Agarwal, S.; Zhou, X.; Ye, F.; He, Q.; Chen, G.C.; Soo, J.; Boey, F.; Zhang, H.; Chen, P.; *Langmuir* **2010**, *26*, 2244. DOI: [10.1021/la9048743](https://doi.org/10.1021/la9048743)

38. Chen, H.; Müller, M.B.; Gilmore, K.J.; Wallace, G.G.; Li, D.; Adv. Mater., **2008**, 20, 3557.
DOI: [10.1002/adma.200800757](https://doi.org/10.1002/adma.200800757)
39. Hu, W.; Peng, C.; Luo, W.; Lv, M.; Li, X.; Li, D.; Huang, Q.; Fan, C.; Acs Nano **2010**, 42, 4317.
DOI: [10.1021/nn101097v](https://doi.org/10.1021/nn101097v)
40. Zhang, R.; Hummelgård, M.; Lv, G.; Olin, H.; Carbon **2011**, 49, 1126.
DOI: [10.1016/j.carbon.2010.11.026](https://doi.org/10.1016/j.carbon.2010.11.026)
41. Kim, I.Y.; Park, S.; Kim, H.; Park, S.; Ruoff, R.S.; Hwang, S.J.; Adv. Funct. Mater., **2014**, 24, 2288.
DOI: [10.1002/adfm.201303040](https://doi.org/10.1002/adfm.201303040)
42. Hummers Jr, W.S.; Offeman, R.E.; J. Am. Chem. Soc., **1958**, 80, 1339.
DOI: [10.1021/ja01539a017](https://doi.org/10.1021/ja01539a017)
43. Marciano, D.C.; Kosynkin, D.V.; Berlin, J.M.; Sinitskii, A.; Sun, Z.; Slesarev, A.; Alemany, L.B.; Lu, W.; Tour, J.M.; ACS nano **2010**, 4, 4806.
DOI: [10.1021/nn1006368](https://doi.org/10.1021/nn1006368)
44. Shen, X.; Lin, X.; Yousefi, N.; Jia, J.; Kim, J.-K.; Carbon **2014**, 66, 84.
DOI: [10.1016/j.carbon.2013.08.046](https://doi.org/10.1016/j.carbon.2013.08.046)
45. Stankovich, S.; Dikin, D.A.; Dommett, G.H.B.; Kohlhaas, K.M.; Zimney, E.J.; Stach, E.A.; Piner, R.D.; Nguyen, S.T.; Ruoff, R.S.; Nature **2006**, 442, 282.
DOI: [10.1038/nature04969](https://doi.org/10.1038/nature04969)
46. Titelman, G.; Gelman, V.; Bron, S.; Khalfin, R.; Cohen, Y.; Bianco-Peled, H.; Carbon **2005**, 43, 641.
DOI: [10.1016/j.carbon.2004.10.035](https://doi.org/10.1016/j.carbon.2004.10.035)
47. Hontoria-Lucas, C.; Lopez-Peinado, A.; López-González, J.d.D.; Rojas-Cervantes, M.L.; Martín-Aranda, R.M.; Carbon **1995**, 33, 1585.
DOI: [10.1016/0008-6223\(95\)00120-3](https://doi.org/10.1016/0008-6223(95)00120-3)
48. Szabó, T.; Berkesi, O.; Dékány, I.; Carbon **2005**, 43, 3186.
DOI: [10.1016/j.carbon.2005.07.013](https://doi.org/10.1016/j.carbon.2005.07.013)
49. Agnihotri, S.A.; Jawalkar, S.S.; Aminabhavi, T.M.; Eur. J. Pharm. Biopharm., **2006**, 63, 249.
DOI: [10.1016/j.ejpb.2005.12.008](https://doi.org/10.1016/j.ejpb.2005.12.008)
50. Basaldella, E.I.; Legnoverde, M.S.; J. Sol-Gel Sci. Technol., **2010**, 56, 191.
DOI: [10.1007/s10971-010-2293-7](https://doi.org/10.1007/s10971-010-2293-7)
51. Uddin, M.N.; Huang, Z.-D.; Mai, Y.-W.; Kim, J.-K.; Carbon **2014**, 77, 481.
DOI: [10.1016/j.carbon.2014.05.053](https://doi.org/10.1016/j.carbon.2014.05.053)
52. Liu, S.; Zeng, T.H.; Hofmann, M.; Burcombe, E.; Wei, J.; Jiang, R.; Kong, J.; Chen, Y.; Acs Nano **2011**, 5, 6971.
DOI: [10.1021/nn202451x](https://doi.org/10.1021/nn202451x)
53. Wang, X.; Zhou, N.; Yuan, J.; Wang, W.; Tang, Y.; Lu, C.; Zhang, J.; Shen, J.; J. Mater. Chem., **2012**, 22, 1673.
DOI: [10.1039/C1JM13360H](https://doi.org/10.1039/C1JM13360H)
54. M.-Y. Lima, Y.-S. Choia, J. Kima, K. Kima, H. Shina, J.-J. Kima, D. Shinb, J.-C. Leea, J. Membr. Sci., **2017**, 521, 1.
DOI: [10.1016/j.memsci.2016.08.067](https://doi.org/10.1016/j.memsci.2016.08.067)
55. J. D. Mangadlao, C. M. Santos, M. J. L. Felipe, a. C. C. de Leon, D. F. Rodrigues, R. C. Advincola, Chem. Commun., **2015**, 51, 2886.
DOI: [10.1039/C4CC07836E](https://doi.org/10.1039/C4CC07836E)
56. J. Chen, X. Zhang, H. Cai, Z. Chen, T. Wang, L. Jia, J. Wang, Q. Wang, X. Pei, Colloids Surf., B, **2016**, 147, 397.
DOI: [10.1016/j.colsurfb.2016.08.023](https://doi.org/10.1016/j.colsurfb.2016.08.023)
57. Z. Marková, K.M. n. Šišková, J. Filip, J. Čuda, M. Kolář, K. r. Šafářová, I. Medřík, R. Zbořil, Environ. Sci. Technol., **2013**, 47, 5285.
DOI: [10.1039/C1JM13360H](https://doi.org/10.1039/C1JM13360H)
58. A. Ahmad, A. Sattar, L. Li, J. Bao, J. Xin, Y. Xu, X. Guo., Colloids Surf., B, **2016**, 143, 490.
DOI: [10.1021/es304693g](https://doi.org/10.1021/es304693g)
59. Ji N, L.; Zeng, Z.; Kuddannaya, S.; Yue, D.; Bao, J.; Wang, Z.; Zhang, Y.; J. Mater. Chem. B **2015**, 3, 4338.
DOI: [10.1039/C5TB00295H](https://doi.org/10.1039/C5TB00295H)



A Monthly Journal

Publish your article in this journal

Advanced Materials Letters is an official international journal of International Association of Advanced Materials (IAAM, www.iaamonline.org) published monthly by VBRI Press AB from Sweden. The journal is intended to provide high-quality peer-review articles in the fascinating field of materials science and technology particularly in the area of structure, synthesis and processing, characterisation, advanced-state properties and applications of materials. All published articles are indexed in various databases and are available download for free. The manuscript management system is completely electronic and has fast and fair peer-review process. The journal includes review article, research article, notes, letter to editor and short communications.

Copyright © 2017 VBRI Press AB, Sweden

www.vbripress.com/aml

Supporting Information

Experimental section

Cell viability assay

Cell viability was evaluated using the standard MTT assay proto-col. HeLa Cells were seeded in 96-well plates and grown overnight prior to studies. Then cells of ~80% confluent were incubated with fresh media containing GO or GO-CE suspensions (0, 25, and 50 $\mu\text{g mL}^{-1}$) at 37 °C for 24 h, 72 h. After each interval, MTT at a concentration of 5 mg mL^{-1} was added to each well and the cells were incubated for 4 h. Upon removal of the MTT solution, the formed crystals were solubilized within isopropanol for 15 min. After centrifugation, the absorbance of the supernatants was measured at 490 nm by using a microplate reader (Infinite M200 Pro, Switzerland).

Cellular morphology on the GO-CE surface was visualized using SEM. Briefly, HeLa Cells were cultured on the GO-CE film incubated at 37 °C in 5 vol% CO_2 for 48 h. The specimens were then gently washed 3 times with PBS solution and fixed with 2.5 wt% glutaraldehyde solution for 120 min followed by dehydration through a graded series of ethanol/water solutions (25 wt%, 35 wt%, 50 wt%, 70 wt%, 80 wt%, 90 wt% and absolute ethanol for 30 min each). Finally, the specimens were vacuum-dried and platinum-coated for SEM study.

Drug release from GO-CE film

The GO-CE film was cut into a circular sheet (diameter = 6 mm) and weighed. Then the specimens were immersed in PBS solution with controlled pH and temperature of 7.4 and 37 °C. The volume of PBS solution was 3 mL for 1 mg specimens. The specimens were immersed in PBS for various times and the solute-ion was analyzed by ultraviolet visible spectroscopy (Shimadzu Co., UV-2550, Japan) at a wavelength of 262 nm. A series concentrations of cefalexin solutions (1~40 $\mu\text{g mL}^{-1}$) were prepared to obtain a linear calibration curve ($R^2 = 0.998$) (Fig. S2†). In order to eliminate any possible interferences of the products, blank solutions for the UV-Vis spectroscopy assay were prepared by collecting leaching solution from the GO film at the same incubation times.

Antibacterial evaluation

Zone of inhibition method

Antibacterial activities of GO and GO-CE films against *S. aureus* and *E. coli* were evaluated using the disc diffusion method. Nutrient agar plates were prepared by dissolving 15 g of agar, 5 g of tryptone, 1 g of glucose, and 2.5 g of yeast extract in 1 L of water. The pH of the solution was then adjusted to 7.0 ± 0.2 . The contents were then sterilized by autoclaving at 120 °C and 0.1 MPa for 30 min. The agar was poured into Petri plates in quantities of 4.5 mL, and left on a flat surface to solidify. The bacteria, in their exponential growth phase, were cultured in the nutrient broth at 37 °C. Then, 50 μL of the bacterial suspension was added drop wise onto the agar medium and dispersed by a triangle glass rod. The GO and GO-CE film were

sterilized by 70 wt% ethanol and cut into a circular sheet (diameter = 6 mm). Then the circular sheets were applied onto the surface of inoculated agar plates. After 24 h of incubation at 37 °C, the culture dishes were examined and recorded.

3.2. Effect of GO-CE drug release solutions on antibacterial activity

GO and GO-CE films were sterilized by 70 wt% ethanol and cut into a circular sheet (diameter = 6 mm). Then the circular sheets were immersed in 3 mL of PBS solution with controlled pH and temperature of 7.4 and 37 °C. The drug release solutions were obtained by taking 100 μL solutions at various times (1 h, 12 h and 24 h). For antibacterial tests, 50 μL of the *S. aureus* suspensions were mixed with 50 μL of drug release solutions and drop wise onto the agar medium and dispersed by a triangle glass rod. For controlled trial, 50 μL of the *S. aureus* suspensions were mixed with 50 μL of PBS solution (pH = 7.4) and then followed the same procedures. After 24 h of incubation at 37 °C overnight, the numbers of colony forming units on agar medium were recorded. Antibacterial activity of drug release solutions were evaluated by:

$$\text{Bacterial Reduction (\%)} = \frac{B - A}{A} \cdot 100 \quad (1)$$

where, A and B are colony forming units of bacteria for the experimental group and control group.

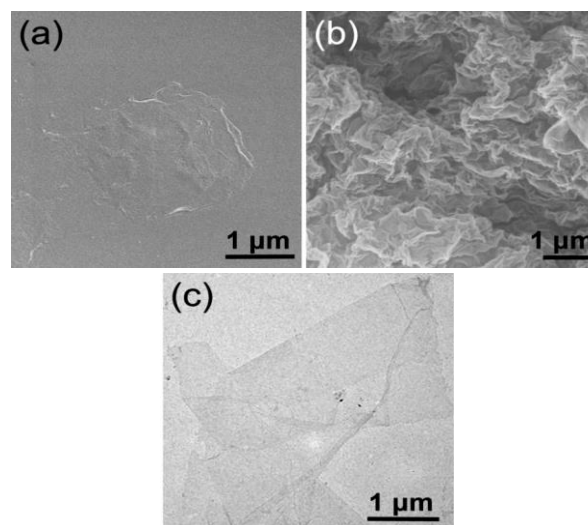


Fig. S1. Morphology of GO sheets. SEM images of GO sheets (a) and (b), TEM image of GO sheets (c).

For scanning electron microscopy (SEM), GO samples were imaged using a Zeiss SIGMA microscope (Germany). About 0.05 mg mL^{-1} GO suspension was dropped on a silicon wafer and dried in a vacuum oven at room temperature for 24 h. Then the silicon wafer was platinum coated and imaged to get a tile image of GO (Fig. S1 (a)). SEM image of agglomeration of GO was shown in (Fig. S1 (b)). For transmission electron microscopy (TEM) observation, 0.01 mg mL^{-1} GO suspension was casted onto lacey carbon supported TEM grids. TEM was carried out on a JEM-2100 (Japan)

transmission electron microscope operated at an
accelerating voltage of 200 kV.